

## Effect of biaxial strain on exciton luminescence of heteroepitaxial ZnSe layers

K. Ohkawa, T. Mitsuyu, and O. Yamazaki

Central Research Laboratories, Matsushita Electric Industrial Company, Ltd., Moriguchi-shi, Osaka 570, Japan

(Received 8 August 1988)

N-doped and Ga-doped ZnSe layers grown by molecular-beam epitaxy on GaAs substrates exhibited double peaks for both the neutral-acceptor-bound-exciton line ( $I_1$ ) and the neutral-donor-bound-exciton line ( $I_2$ ) in low-temperature photoluminescence measurements. The split energy of the double peaks corresponds to an activation energy derived from the Arrhenius plot of intensity ratio of the double peak. Peak energies of the double peaks are calculated from energy shifts of valence bands split by biaxial strain, produced by lattice mismatch and differences in thermal contraction between ZnSe and GaAs. These indicate that the double peak of both bound-exciton lines was yielded from two kinds of excitons related to a light hole and a heavy hole of the valence bands. Thus it should be pointed out that the  $I_x$  line generally reported in  $n$ -type ZnSe heteroepitaxial layers corresponds to a light-hole branch of usual  $I_2$  line.

### I. INTRODUCTION

Lattice mismatch and difference in thermal expansion coefficients greatly affect the properties of heteroepitaxially grown semiconductor thin films and superlattices. Investigation of these effects is necessary for understanding the fundamentals of heteroepitaxy and their application for heterojunction.

GaAs has been widely used as a substrate for ZnSe epitaxial growth, because of a small lattice mismatch of 0.28% at room temperature. This lattice mismatch of a small amount, however, influences the early stage of ZnSe epitaxial growth. X-ray diffraction measurements shows that the thin ZnSe layer is coherently grown on a GaAs substrate with tetragonal distortion.<sup>1,2</sup> With increasing layer thickness, the lattice parameter perpendicular to the heterointerface ( $a_{\perp}$ ) approaches the lattice parameter of bulk ZnSe, indicating a relaxation of the mismatch distortion. The lattice parameter  $a_{\perp}$  becomes smaller than the bulk value for layers thicker than 1–1.5  $\mu\text{m}$ . Yao *et al.* have indicated that the thick layers suffer biaxial tensile stress produced by differences in thermal contraction between ZnSe and GaAs on cooling below the growth temperature.<sup>2</sup>

The strain produced by the lattice mismatch and the differential thermal contraction have influences not only on crystallinity but also on photoluminescence properties of heteroepitaxial ZnSe layers.<sup>2–6</sup> Homoepitaxial ZnSe layers and ZnSe single crystals exhibit a single bound-exciton line with both a donor and an acceptor origin.<sup>7,8</sup> In the case of ZnSe layers on GaAs substrates, a new  $I_x$  line appears at a lower energy position than the  $I_2$  line.<sup>9</sup> It has been believed that the donor of the  $I_x$  line is different from that of the  $I_2$  line.<sup>2,9</sup> The dominant bound-exciton luminescence was observed in our N-doped and Ga-doped ZnSe layers on GaAs substrates, as shown in Fig. 1. In this paper we will present the effect of the strain on the bound-exciton luminescence, and point out that the  $I_x$  line is a branch of the  $I_2$  line caused

by the strain; a similar effect is also observed for the neutral-acceptor-bound-exciton line.

### II. GROWTH OF ZnSe LAYERS

GaAs substrates used are undoped, semi-insulating, and (100) oriented. Treatment of the GaAs substrates for cleaning were described in a previous publication.<sup>10</sup> Ga-doped ZnSe layers were grown by molecular-beam epitaxy (MBE) with high-purity Zn, Se, and Ga beams. The doping level of Ga was controlled by the temperature of the Knudsen cell containing Ga. Carrier concentration of the Ga-doped ZnSe layers is less than  $1 \times 10^{17} \text{ cm}^{-3}$ . N-doped ZnSe layers were grown by MBE with Zn, Se, and low-energy nitrogen-ion beams. We used an ion-gun system with a mass separator to make a high-purity  $\text{N}_2^+$  molecular-ion beam for nitrogen doping. The ion energy was on order of  $10^2 \text{ eV}$ , and the ion current density at the substrate was less than  $0.5 \text{ nA/cm}^2$ . Details of the growth procedure of the N-doped ZnSe layers were described in Ref. 11. The substrate temperature during growth was kept at  $325^\circ\text{C}$ . The beam flux ratio of Zn to Se was approximately  $J_{\text{Zn}}/J_{\text{Se}} = 1$ . The growth rate was  $0.5\text{--}0.7 \mu\text{m/h}$ . The layer thicknesses are in the range  $0.05\text{--}5 \mu\text{m}$ .

### III. PHOTOLUMINESCENCE PROPERTIES

The photoluminescence (PL) properties were measured in a temperature range from 4.2 K to room temperature. The PL was exciting using 325-nm emission from a He-Cd laser. The excitation power density was as low as  $0.5 \text{ W/cm}^2$ .

Low-temperature PL spectra of typical undoped, N-doped, and Ga-doped ZnSe layers are shown in Fig. 1. The PL spectrum of the undoped ZnSe layer exhibits strong free-exciton emission ( $E_x$ ) with weak donor-bound-exciton emission and suppressed deep-level emission. This indicates high crystalline quality and high purity of our ZnSe layer. The PL spectra of the N-doped

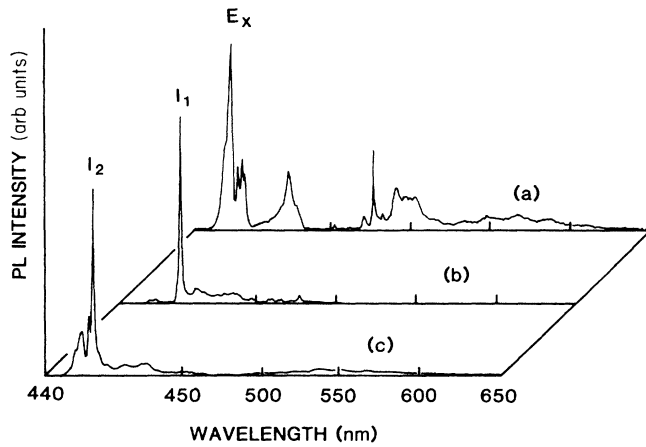


FIG. 1. Photoluminescence spectrum of (a) undoped ZnSe layers on GaAs is measured at 12 K, (b) those of N-doped, and (c) Ga-doped ZnSe layers are measured at 4.2 K.

and Ga-doped ZnSe layers exhibit strong bound-exciton lines ( $I_1$  and  $I_2$  lines, respectively) with the  $E_x$  line. These PL spectra indicate that acceptors and donors in these doped ZnSe layers are very active and do not create deep centers. Figure 2 shows PL spectra in the excitonic emission region for the N-doped ZnSe layer at different temperatures. The  $E_x$  line and the dominant-acceptor-bound-exciton line at 2.790 eV are observed in the spectrum at 4.2 K. An upper energy line at 2.792 eV grows upward with an increase of temperature. Here, we call the acceptor-bound-exciton line at 2.790 eV the  $I_1^l$  line; the upper energy line at 2.792 eV, the  $I_1^h$  line; the customary  $I_2$  line, the  $I_2^h$  line; and the customary  $I_x$  line, the  $I_2^l$  line.

Figure 3 shows band structures of ZnSe near the  $\Gamma$  point under unstrained and strained conditions. The valence band at the  $\Gamma$  point of the unstrained ZnSe layer consists of a fourfold  $P_{3/2}$  multiplet ( $J = \frac{3}{2}$ ,  $m_J = \pm\frac{3}{2}, \pm\frac{1}{2}$ ). Under biaxial compressive or tensile

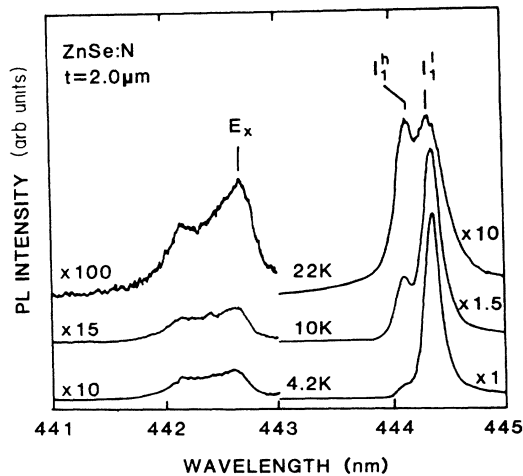


FIG. 2. Temperature dependence of the excitonic emission PL spectra of N-doped ZnSe with layer thickness 2.0  $\mu\text{m}$ .

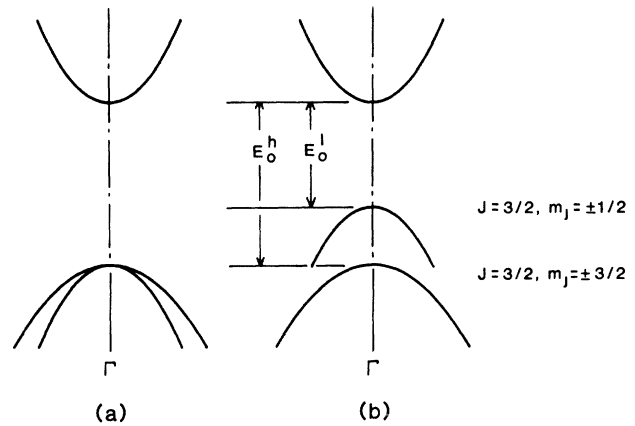


FIG. 3. Schematic representation of (a) unstrained band structure and (b) biaxial tensile-stressed band structure.

stress parallel to  $[010]$  and  $[001]$ , the valence band is split into a heavy-hole branch ( $J = \frac{3}{2}$ ,  $m_J = \pm\frac{3}{2}$ ) and a light-hole branch ( $J = \frac{3}{2}$ ,  $m_J = \pm\frac{1}{2}$ ).<sup>5,6</sup> The  $I_1^h$  and  $I_2^h$  lines might be luminescence from bound excitons consisting of a heavy hole and an electron, and the  $I_1^l$  and  $I_2^l$  lines might be luminescence from bound excitons consisting of a light hole and an electron.

The Arrhenius plots of the PL intensity ratio  $I_1^l/I_1^h$  and  $I_2^l/I_2^h$  are shown in Fig. 4. We assume that PL intensities of the  $I_1^h$  (or  $I_2^h$ ) line and the  $I_1^l$  (or  $I_2^l$ ) line are in proportion to populations of heavy and light holes in the

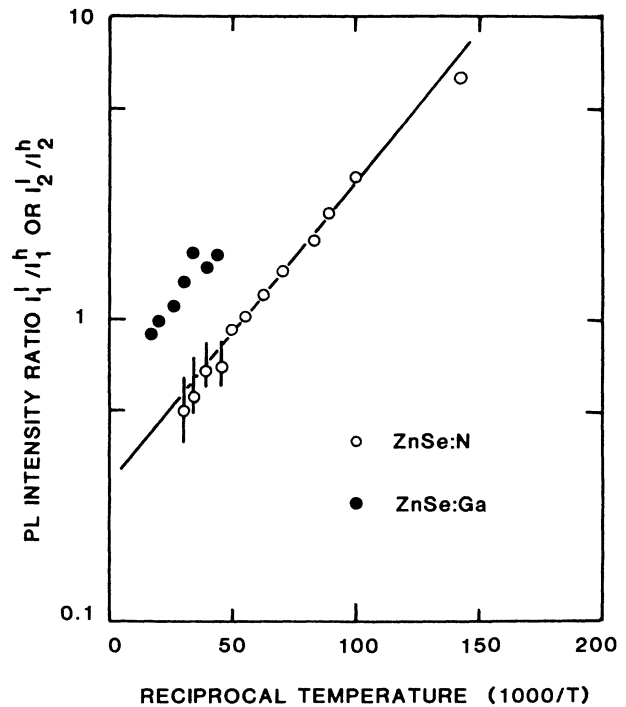


FIG. 4. Temperature dependence of ratio  $I_1^l/I_1^h$  and  $I_2^l/I_2^h$ . Thicknesses of the N-doped and Ga-doped ZnSe layers are 2.0 and 4.8  $\mu\text{m}$ , respectively. Solid line has activation energy 2 meV.

split valence bands, respectively, and that the transition possibility of exciton recombination corresponding to a heavy hole is  $A$  ( $=\text{const}$ ) times larger than that of a light hole. These assumptions are shown in equations  $I^h \propto AN^h$  and  $I^l \propto N^l$  where  $I^h$  and  $I^l$  are PL intensities for the heavy-hole branch and the light-hole branch, respectively, and  $N^h$  and  $N^l$  are populations of heavy and light holes, respectively. Then the Arrhenius equation is

$$I^l/I^h = \exp(E_a/kT)/A, \quad (1)$$

where  $E_a$  is an activation energy. The plot of the ratio  $I_1^l/I_1^h$  in Fig. 4 gives  $A=3.5$  and  $E_a=2$  meV. In the case of the ratio  $I_2^l/I_2^h$ ,  $A=1.5$  and  $E_a=2$  meV were obtained. It could be pointed out that the activation energy  $E_a$  equals the split energy of the  $I_1^h$  line (2.792 eV) and the  $I_1^l$  line (2.790 eV) in Fig. 2. This result reveals that origins of  $I^h$  and  $I^l$  have the same impurity species and that a hole is thermally excited from a lower-energy state to a higher-energy state. The ratio  $I^l/I^h$  depends on the  $E_a$  and temperature from Eq. (1). As the split energy between the  $I_1^l$  line and the  $I_1^h$  line is almost constant for layers thicker than  $1.5 \mu\text{m}$  as shown in Fig. 7,  $E_a$  is constant for thick layers and the ratio depends only on temperature. Thus the ratio  $I^l/I^h$  would be useful as a temperature monitor of a sample whose temperature is uncertain. The ratios  $I^l/I^h$  of various samples are constant at a given temperature as shown in Fig. 5 and the ratio  $I^l/I^h$  is about 1.8 in thick N-doped ZnSe layers at 12 K and also in thick Ga-doped ZnSe layers at 4.2 K. This proportional relation of  $I_2$  ( $=I_2^h$ ) and  $I_x$  ( $=I_2^l$ ) also suggests that  $I_2$  and  $I_x$  originate from same donor species.

#### IV. LAYER-THICKNESS DEPENDENCE OF LATTICE PARAMETERS

Strain in the layer can be evaluated by a measurement of lattice parameter or a Raman scattering measure-

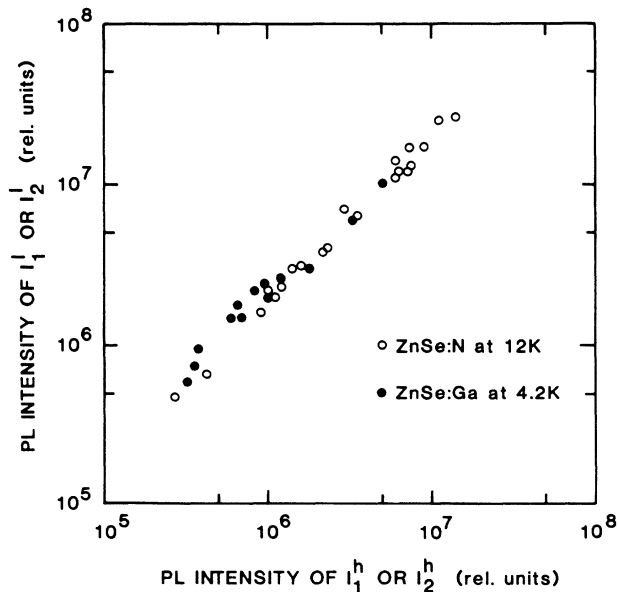


FIG. 5. Plots of intensities of  $I_1^l$  vs  $I_1^h$  and  $I_2^l$  vs  $I_2^h$  of ZnSe layers with various layer thicknesses ( $1.5$ – $5 \mu\text{m}$ ).

ment.<sup>12</sup> We measured the lattice parameter  $a_{\perp}$  [which is perpendicular to the (100) heterointerface] of ZnSe layers. Figure 6 shows the  $a_{\perp}$  of ZnSe layers plotted as a function of layer thickness at room temperature and 12 K. The  $a_{\perp}$  at room temperature is an experimental value, but the  $a_{\perp}$  at 12 K is a calculated value. It is necessary to know low-temperature strain for the investigation of its influence on the low-temperature PL properties.

We postulate the following mechanism of the heteroepitaxy to calculate the  $a_{\perp}$  at 12 K, and define three states of temperatures: the growth temperature ( $325^{\circ}\text{C}$ ) state, the room-temperature state for the x-ray diffraction measurement, and the low-temperature (12 K) state for the PL measurement. During the growth temperature, the layer of the early stage is coherently grown and tetragonally deformed by compressive stress due to the lattice mismatch.<sup>1,6,13,14</sup> As dislocations are induced after growing this thin coherent layer, the lattice structure of ZnSe will change into cubic gradually. At the room temperature the layer is biaxially stretched, since the cubic structure of thick layers at the growth temperature suffers tensile stress due to the differences in thermal contraction between ZnSe and GaAs on cooling below the growth temperature. This stress reflects that the  $a_{\perp}$  of thick layers becomes smaller than that of bulk ZnSe. We can calculate the lattice parameter of ZnSe layers at 12 K by the above mechanism for the heteroepitaxy.

The  $a_{\perp}$  of thin, i.e., coherent, ZnSe layers on the GaAs substrate is given by<sup>1,5</sup>

$$a_{\perp} = a_{\text{GaAs}} + \frac{C_{11} + 2C_{12}}{C_{11}}(a_{\text{bulk}} - a_{\text{GaAs}}), \quad (2)$$

where  $C_{11}$  and  $C_{12}$  are the elastic stiffness constants of

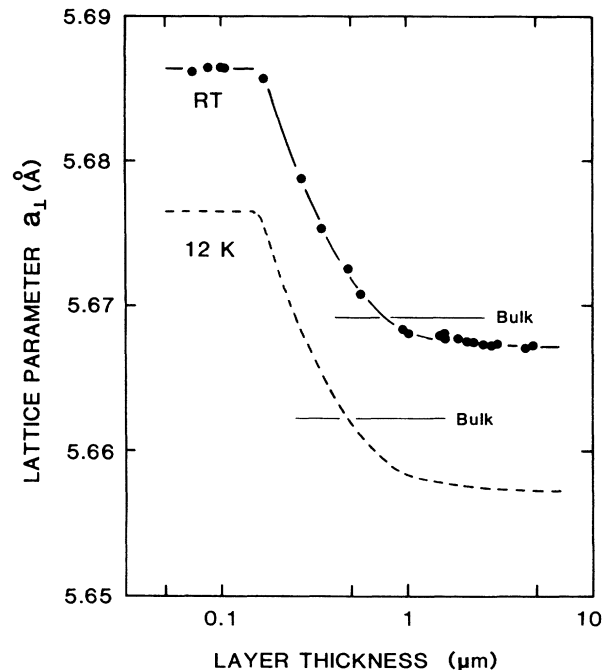


FIG. 6. Lattice parameter  $a_{\perp}$  of ZnSe layers plotted as functions of layer thickness at room temperature and at 12 K.

ZnSe and the  $a_{\text{bulk}}$  is the lattice parameter of bulk ZnSe. Using  $C_{11}, C_{12}$  in Table I, we can evaluate the lattice parameter  $a_{\perp} = 5.688 \text{ \AA}$  of the coherent ZnSe layers at 300 K. This value is in quite good agreement with our experimental value of  $a_{\perp} = 5.687 \text{ \AA}$  at room temperature and other experimental values.<sup>1,14</sup> In this case the ZnSe lattice parameter  $a_{\parallel}$  (which is parallel to the heterointerface) takes the value of the GaAs lattice parameter.

Influence of the differential thermal contraction is remarkable on lattice parameters of thick ( $t > 1 \mu\text{m}$ ) ZnSe layers. At the growth temperature, the lattice parameter for regions away from the interface of the thick layer would have the bulk value. On cooling below the growth temperature, change of the  $a_{\parallel}$  would be fixed on that of the GaAs lattice parameter. These assumption can give an equation as follows:

$$\frac{a_{\text{GaAs}}(300 \text{ K}) - a_{\text{GaAs}}(600 \text{ K})}{a_{\text{GaAs}}(600 \text{ K})} = \frac{a_{\parallel}(300 \text{ K}) - a_{\text{bulk}}(600 \text{ K})}{a_{\text{bulk}}(600 \text{ K})}. \quad (3)$$

Then, it gives  $a_{\parallel}(300 \text{ K}) = 5.674 \text{ \AA}$  for thick layers. We can exchange  $a_{\text{GaAs}}$  for  $a_{\parallel}$  in Eq. (2), then  $a_{\perp}(300 \text{ K}) = 5.665 \text{ \AA}$  for thick layers is obtained. This calculated  $a_{\perp}(300 \text{ K})$  for thick layers is in good agreement with experimental value of  $5.667 \text{ \AA}$ , as shown in Fig. 6.

We calculated  $a_{\perp}$  at 12 K for thin and thick ZnSe layers using these procedures. The  $a_{\perp}(12 \text{ K})$  calculated are  $5.679$  and  $5.655 \text{ \AA}$  for thin and thick ZnSe layers, respectively. In addition, we assume that the manner of lattice parameter relaxation at moderate thickness is identical for 12 and 300 K, and that a difference between the calculated value and experimental value is also identical for both temperatures. Thus, the lattice parameter  $a_{\perp}(12 \text{ K})$  is plotted as a function of layer thickness in Fig. 6 (dashed line).

## V. DISCUSSION

For the case of zinc-blende-type material, band-gap shifts at the  $\Gamma$  point with biaxial stress are given by<sup>4,5</sup>

$$\begin{aligned} \Delta E_0^h &= -2a \frac{C_{11} - C_{12}}{C_{11}} \epsilon + b \frac{C_{11} + 2C_{12}}{C_{11}} \epsilon, \\ \Delta E_0^l &= -2a \frac{C_{11} - C_{12}}{C_{11}} \epsilon - b \frac{C_{11} + 2C_{12}}{C_{11}} \epsilon. \end{aligned} \quad (4)$$

Here  $\Delta E_0^h$  and  $\Delta E_0^l$  are energy shifts of the band gaps between conduction and valence bands concerned with the heavy- and the light-hole branches, respectively,  $a$  is the hydrostatic deformation potential,  $b$  is the shear deformation potential, and  $\epsilon$  is the magnitude of the strain component. The  $\epsilon$  is defined to be positive for compressive strain. Inserting  $a = -3.0 \text{ eV}$ ,  $b = -1.2 \text{ eV}$  (Ref. 15), and the values of Table I, we obtain the following results at 12 K:

$$\begin{aligned} \Delta E_0^h &= -0.19\epsilon \text{ eV}, \\ \Delta E_0^l &= 5.06\epsilon \text{ eV}. \end{aligned} \quad (5)$$

These equations show features in band-gap shifts. The energy shift of the heavy-hole branch of the valence bands is almost independent of the strain, but the energy shift of the light-hole branch is fairly dependent on the strain. For the biaxial stress parallel to the heterointerface, nonzero components of the strain tensor are<sup>5,16</sup>

$$\begin{aligned} \epsilon &= -\epsilon_{xx} = -\epsilon_{yy} = \frac{C_{11}}{2C_{12}} \epsilon_{zz}, \\ \epsilon_{zz} &= \frac{a_{\perp} - a_{\text{bulk}}}{a_{\text{bulk}}}. \end{aligned} \quad (6)$$

We can derive the strain in ZnSe layers by inserting the lattice parameter  $a_{\perp}$  at 12 K in Fig. 6. For example, strains in thin ( $t < 0.15 \mu\text{m}$ ) and thick ( $t > 2 \mu\text{m}$ ) layers are  $2.13 \times 10^{-3}$  and  $-7.89 \times 10^{-4}$ , respectively. The point where  $\epsilon = 0$  is around  $0.5 \mu\text{m}$ . The difference between  $a_{\perp}$  and  $a_{\text{bulk}}$  in the thick region at 12 K is much larger than the difference at room temperature, as shown in Fig. 6. Effects of the strain produced by the differential thermal contraction cannot be ignored at low temperature.

TABLE I. Values of lattice parameters of ZnSe and GaAs, and of elastic stiffness constants for ZnSe at three temperatures (12, 300, and 600 K).

Temp. (K)	Lattice parameters of bulk (\AA)		Elastic stiffness constants of ZnSe ( $10^{11} \text{ dyn/cm}^2$ )	
	GaAs	ZnSe	$C_{11}$	$C_{12}$
600	5.6639 <sup>a</sup>	5.6841 <sup>c</sup>		
300	5.6533 <sup>b</sup>	5.6693 <sup>c</sup>	8.59 <sup>d</sup>	5.06 <sup>d</sup>
12	5.6479 <sup>a</sup>	5.6623 <sup>c</sup>	8.88 <sup>d</sup>	5.27 <sup>d</sup>

<sup>a</sup>Y. S. Touloukian, R. K. Kirby, R. E. Taylor, and T. Y. R. Lee, in *Thermophysical Properties of Matter*, edited by Y. S. Touloukian (Plenum, New York, 1977), Vol. 13, p. 747.

<sup>b</sup>J. B. Mullin, B. W. Straughan, C. M. H. Driscoll, and A. F. W. Willoughby, in *Institute of Physics Conference Series* (IOP, Bristol, 1975), Vol. 24, p. 275.

<sup>c</sup>H. P. Singh and B. Dayal, *Phys. Status Solidi* **23**, K93 (1967).

<sup>d</sup>B. H. Lee, *J. Appl. Phys.* **41**, 2984 (1970).

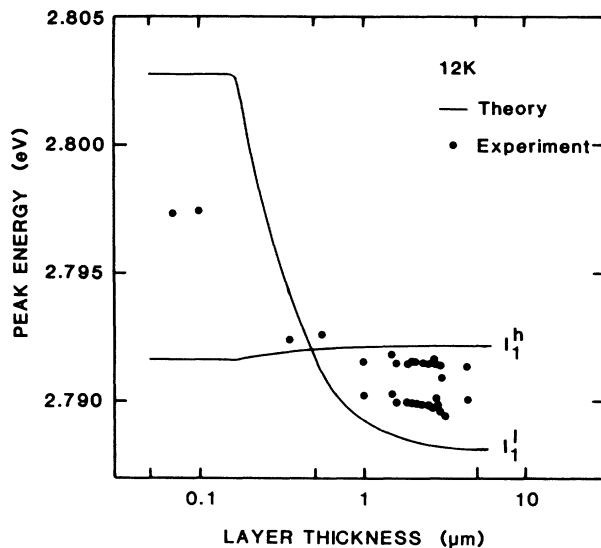


FIG. 7. Variation of excitonic peak energies in the 12-K PL spectra of the N-doped ZnSe layers of varying thickness. Solid lines are calculated peak energies of the  $I_1^l$  and  $I_1^h$  lines. The  $I_1^h$  line is not discernible in the spectra of thinner layers.

The energy shifts of the valence bands are calculated using Eqs. (5) and (6). It has been reported that a N-doped ZnSe layer homoepitaxially grown by liquid-phase epitaxy, which is free from strain, exhibits the  $I_1$  line at 2.792 eV.<sup>17</sup> The energy shifts of the valence bands were scaled from this peak energy in Fig. 7, and this is the calculated peak energies of the  $I_1^l$  and  $I_1^h$  lines. The peak energy of the  $I_1^l$  shifts to higher energy for thinner ZnSe

layers. The peak shift of  $I_1^h$  is much smaller than that of  $I_1^l$ . The calculated peak energies are in good agreement with the peak energies of the  $I_1^l$  and  $I_1^h$  lines. In addition, similar property was also observed in the  $I_2^l$  and the  $I_2^h$  lines of the Ga-doped ZnSe layers. This result reveals that the  $I_1^l$  and  $I_2^l$  lines are luminescence from the light-hole exciton, and the  $I_1^h$  and  $I_2^h$  lines are luminescence from the heavy-hole exciton.

## VI. SUMMARY

N-doped and Ga-doped ZnSe layers are grown by molecular-beam epitaxy on (100) GaAs substrates. Double peaks in both the  $I_1$  and  $I_2$  lines were observed in the low-temperature PL of the heteroepitaxial ZnSe layers. The Arrhenius plots of the PL intensity ratios of both these two peaks exhibit that each activation energy of the plots corresponds with the split energy of the double peaks. We calculated the low-temperature lattice parameter to fit the temperature of PL measurements. The valence band is split into heavy- and light-hole branches by the strain. We have demonstrated that calculated peak energies of the double peaks using the split valence bands are in good agreement with the experimental peak energies in various layer thicknesses. In heteroepitaxial semiconductors, both the  $I_1$  and  $I_2$  lines split into heavy- and light-hole branches by the biaxial strain due to lattice mismatch and differences in thermal contraction.

## ACKNOWLEDGMENTS

The authors are grateful to Dr. K. Wasa for supporting this work and to T. Karasawa for useful discussions.

<sup>1</sup>H. Mitsuhashi, I. Mitsuishi, M. Mizuta, and H. Kukimoto, *Jpn. J. Appl. Phys.* **24**, L578 (1985).  
<sup>2</sup>T. Yao, Y. Okada, S. Matsui, K. Ishida, and I. Fujimoto, *J. Cryst. Growth* **81**, 518 (1987).  
<sup>3</sup>H. A. Mar and R. M. Park, *J. Appl. Phys.* **60**, 1229 (1986).  
<sup>4</sup>J. E. Potts, H. Cheng, S. Mohapatra, and T. L. Smith, *J. Appl. Phys.* **61**, 333 (1987).  
<sup>5</sup>H. Asai and K. Oe, *J. Appl. Phys.* **54**, 2052 (1983).  
<sup>6</sup>P. J. Dean, *Phys. Status Solidi A* **81**, 625 (1984).  
<sup>7</sup>K. Menda, I. Takayasu, T. Minato, and M. Kawashima, *J. Cryst. Growth* **86**, 342 (1988).  
<sup>8</sup>M. Isshiki, *J. Cryst. Growth* **86**, 615 (1988).  
<sup>9</sup>T. Yao, Y. Makita, and S. Maekawa, *Jpn. J. Appl. Phys.* **20**, L741 (1981).  
<sup>10</sup>K. Ohkawa, T. Mitsuyu, and O. Yamazaki, *J. Appl. Phys.* **62**, 3216 (1987).

<sup>11</sup>K. Ohkawa, T. Mitsuyu, and O. Yamazaki, *J. Cryst. Growth* **86**, 329 (1988).  
<sup>12</sup>O. J. Olego, K. Shahzad, J. Petruzzello, and D. Cammack, *Phys. Rev. B* **36**, 7674 (1987).  
<sup>13</sup>J. Kleiman and R. M. Park, *J. Appl. Phys.* **61**, 2067 (1987).  
<sup>14</sup>A. Kamata, K. Hirahara, M. Kawachi, and T. Beppu, in *Extended Abstracts of the 17th Conference on Solid State Devices and Materials* (The Japan Society of Applied Physics, Tokyo, 1985), p. 233.  
<sup>15</sup>D. W. Langer and R. N. Euwema, *Phys. Rev. B* **2**, 4005 (1970).  
<sup>16</sup>G. H. Olsen, C. J. Nuese, and R. T. Smith, *J. Appl. Phys.* **49**, 5523 (1978).  
<sup>17</sup>P. J. Dean, W. Stutius, G. F. Neumark, B. J. Fitzpatrick, and R. N. Bhargava, *Phys. Rev. B* **27**, 2419 (1983).